Bioengineering 280A
Principles of Biomedical Imaging

Fall Quarter 2012
MRI Lecture 7

fMRI

MRI studies brain <u>anatomy</u>.

<u>Functional</u> MRI (fMRI) studies brain <u>function</u>.

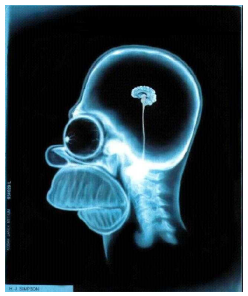

http://defiant.ssc.uwo.ca/Jody_web/fmri4dummies.htm

fMRI Setup

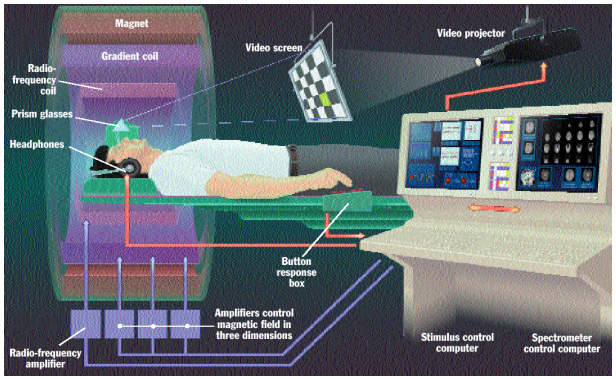

http://defiant.ssc.uwo.ca/Jody_web/fmri4dummies.htm

History of Functional MRI

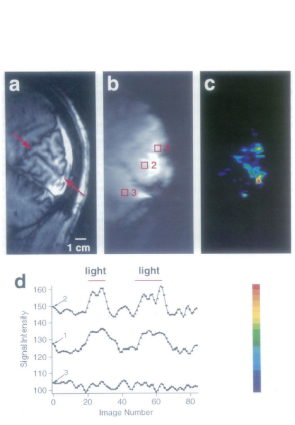

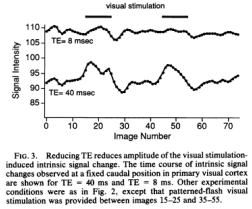

Source: Ogawa et al., 1992

The Rise of fMRI

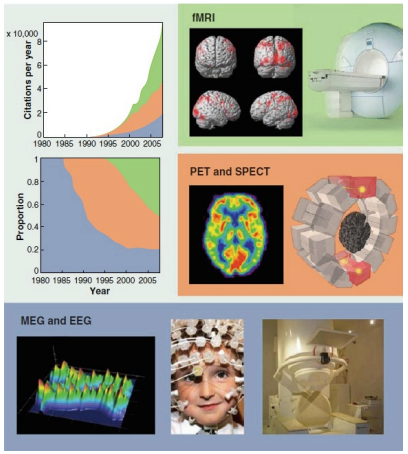

Friston, 2010, Science

What is functional magnetic resonance imaging (fMRI)?

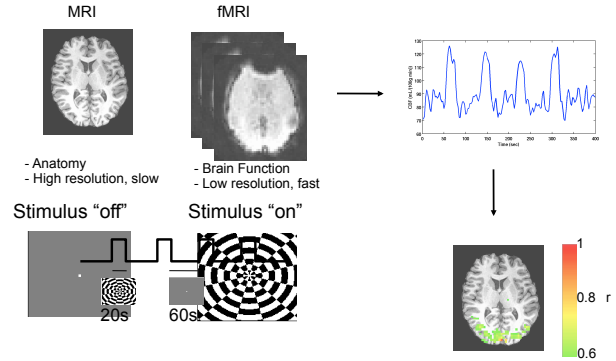

- fMRI provides non-invasive estimates of brain function

Finger Tapping Task

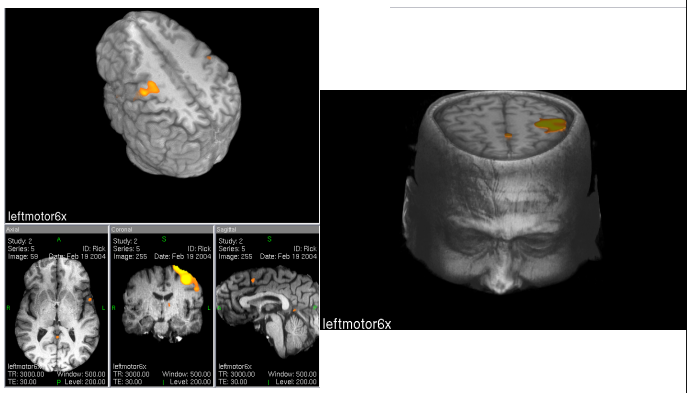

BOLD Signal Change

Baseline Signal

$$S_B = M_0 \exp\left(-TE \cdot R^*_{2,B}\right)$$

Activation Signal

$$S_A = M_0 \exp\left(-TE \cdot R^*_{2,A}\right)$$

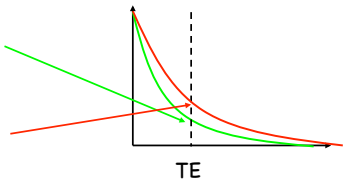

$$\frac{\Delta BOLD}{BOLD_0} = \frac{S_A - S_B}{S_B} \approx -TE \cdot \Delta R^*_2$$

R2* Depends on dHB

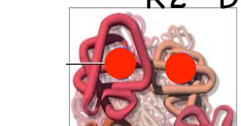

Oxygen binds to the iron atoms to form oxyhemoglobin HbO_2

Release of O_2 to tissue results in deoxyhemoglobin $dHBO_2$

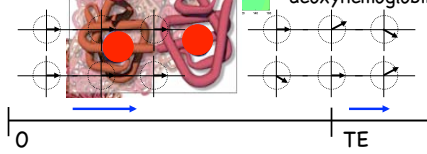

Some dHB, Some dephasing

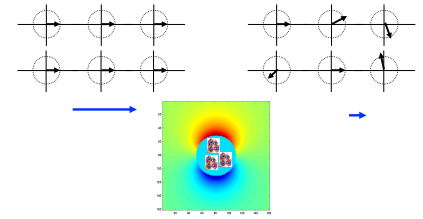

More dHB, More dephasing, Decrease in MR signal

BOLD Signal Equation

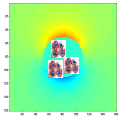

$R^*_{2,dHB} \propto$ Total dHb

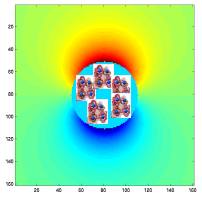

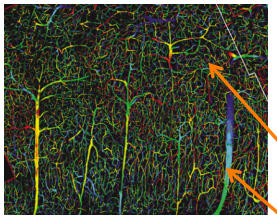

Cassot et al, 2006

$R^*_{2,dHB} = A \cdot CBV \cdot [dHb]^{\beta}_{v}$

Blood Volume

$\beta \approx 2$

$\beta \approx 1$

Simulations suggest $\beta \approx 1.5$ is a reasonable overall value

Ogawa et al, 1993; Boxerman et al 1995, Hoge et al. 1999

Oxygen Extraction

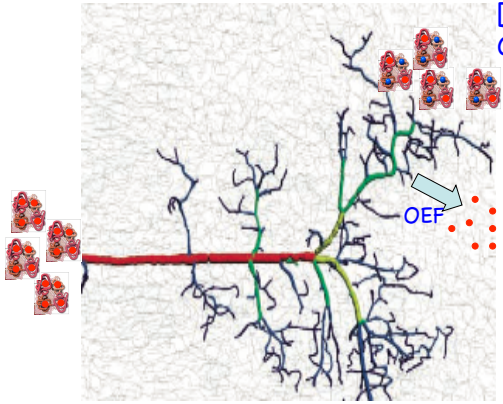

$[dHB]_{venous}$= OEF x $[O_2]_{arterial}$

OEF = Oxygen Extraction Fraction

Cassot et al, 2009

Blood Flow and Oxygen Metabolism

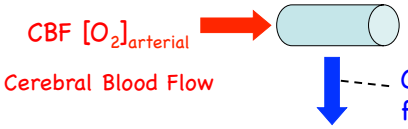

$CMRO_2$= OEF x CBF x $[O_2]_{arterial}$

Deoxyhemoglobin

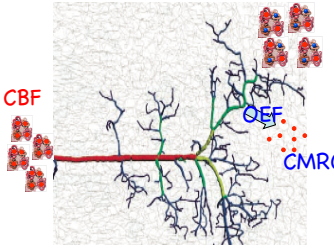

$[dHB]_{venous} = OEF \times [O_2]_{arterial}$

$= CMRO_2/CBF$

Cassot et al, 2009

Blood Flow and Oxygen Metabolism

$[dHb]_{venous} = CMRO_2/CBF$

$CBF\ [O_2]_{arterial}$

Cerebral Blood Flow

Oxygen extraction fraction (OEF)

$CMRO_2$

Cerebral Metabolic Rate of Oxygen

$\uparrow$ CBF $\rightarrow$ $\downarrow [dHB]_{venous}$

$\uparrow CMRO_2 \rightarrow \uparrow [dHB]_{venous}$

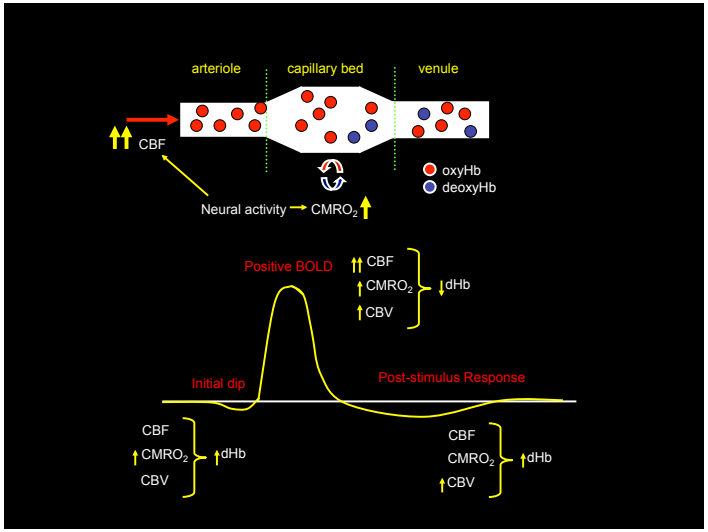

BOLD Signal Path

$R_{2,dHB}^{*} = A\ CBV\ [dHB]^{\beta}_{venous}$

$\approx A\ CBV\ (CMRO_2/CBF)^{\beta}$

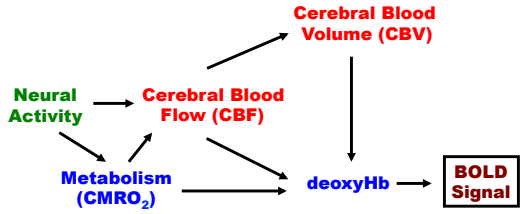

fMRI Acquisition

High spatial resolution | High temporal resolution

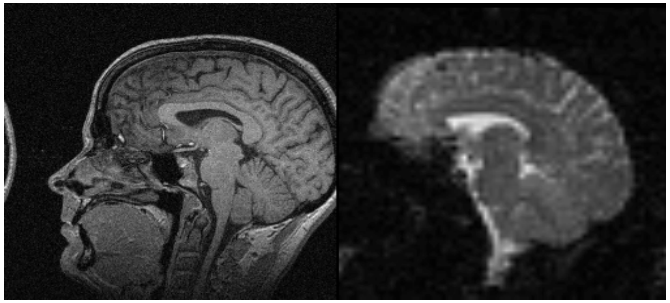

MP-RAGE
Voxel volume: 1 mm^3
Imaging time: 6 min

EPI
Voxel volume: 45 mm^3
Imaging time: 60 msec

Buxton 2002

EPI Scans

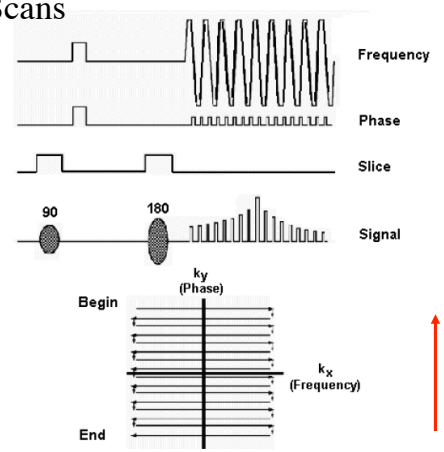

GE Medical Systems 2003

Field Inhomogeneities

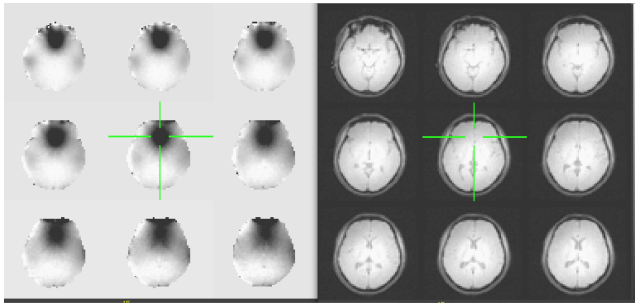

EPI Distortions and Signal Dropouts

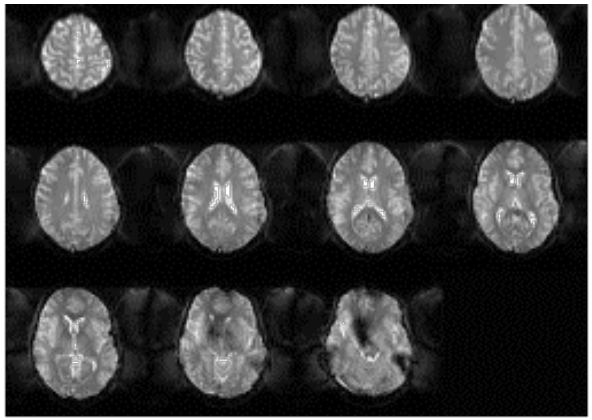

Credit: R. Buxton

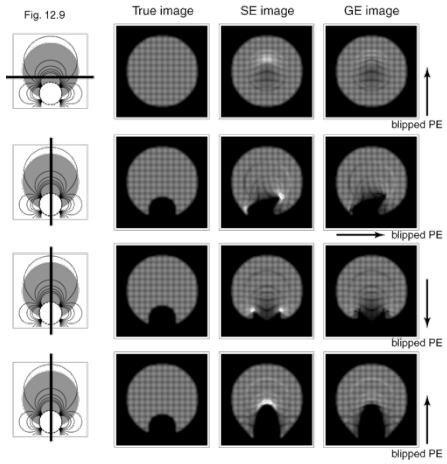

Credit: R. Buxton

Signal Decay

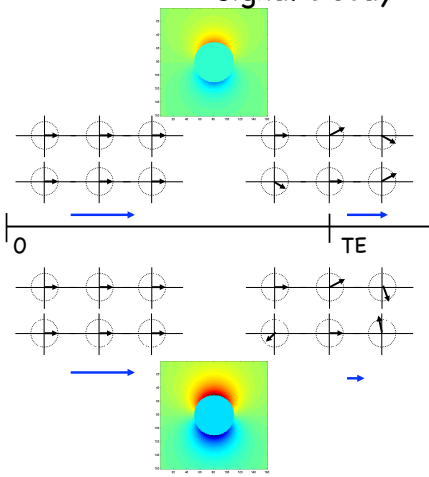

Some inhomogeneity, Some dephasing

More inhomogeneity, More dephasing, Decrease in MR signal

Spin Echo

Discovered by Erwin Hahn in 1950.

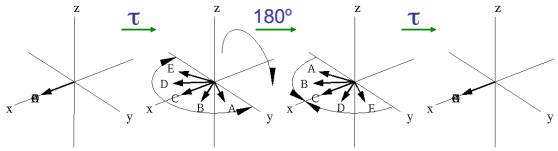

The spin-echo can refocus the dephasing of spins due to static inhomogeneities. However, there will still be T_2 dephasing due to random motion of spins.

There is nothing that nuclear spins will not do for you, as long as you treat them as human beings. Erwin Hahn

Image: Larry Frank

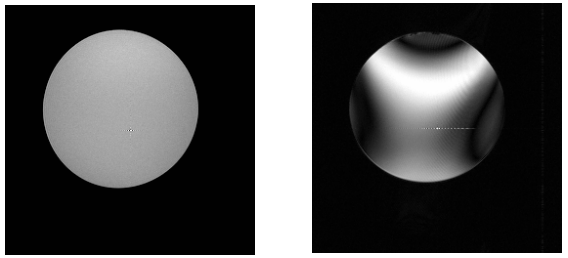

http://chickscope.beckman.uiuc.edu/roosts/carlartifacts.html#Shimming

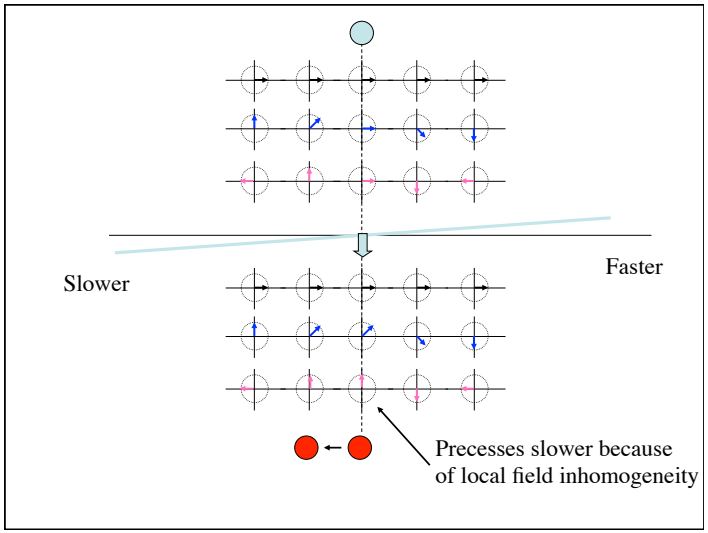

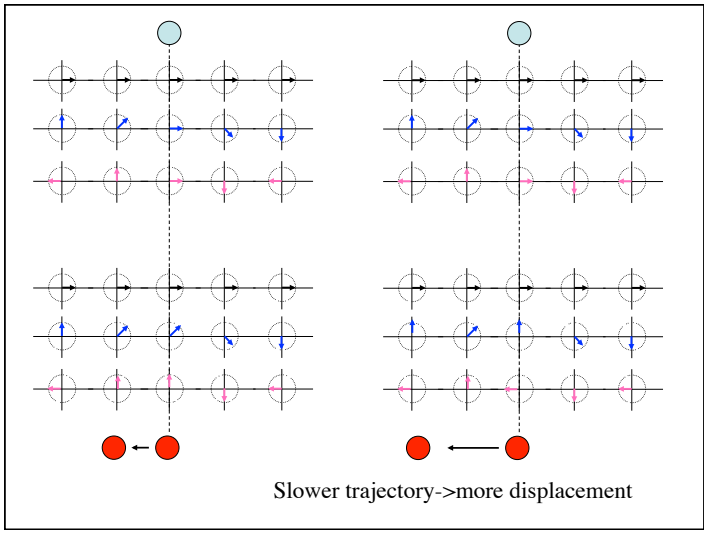

Field Map Correction

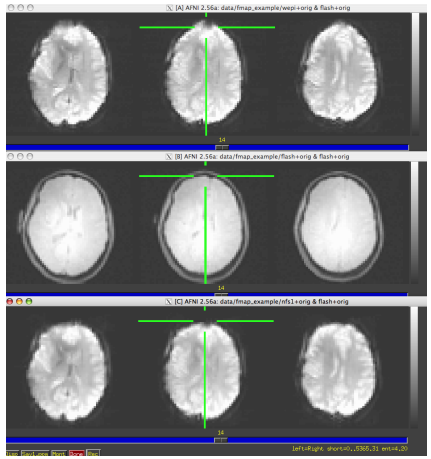

Nyquist Ghosts

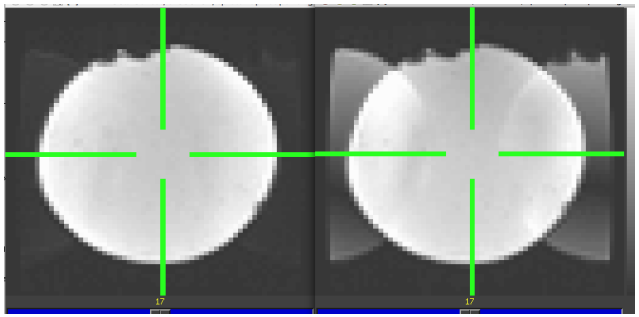

Task-Related BOLD fMRI

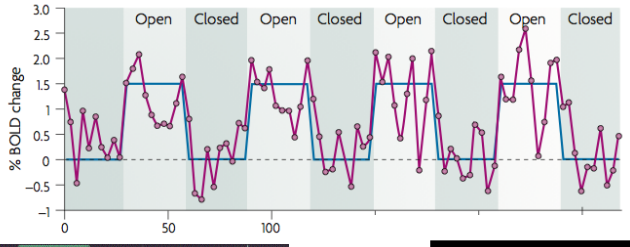

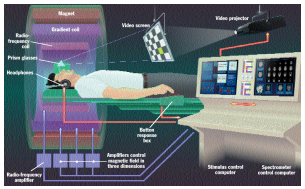

Open – Closed =

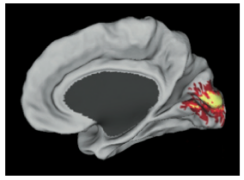

http://defiant.ssc.uwo.ca/Jody_web/fmri4dummies.htm

Fox and Raichle 2007

Task-Related BOLD fMRI

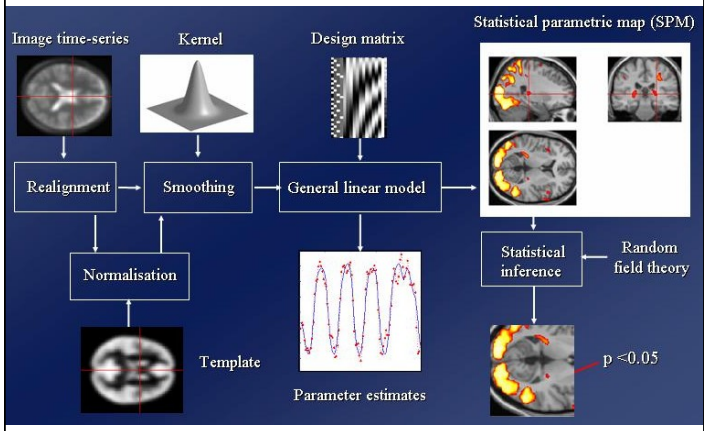

http://www.scholarpedia.org/article/Statistical_parametric_mapping_(SPM)

Functional MRI

Large-amplitude, spatially correlated fluctuations in BOLD fMRI signals during extended rest and early sleep stages

Masaki Fukunaga[a,*], Silvina G. Horovitz[a], Peter van Gelderen[a], Jacco A. de Zwart[a], J. Martijn Jansma[a], Vasiliki N. Ikonomidou[a], Renxin Chu[a], Roel H.R. Deckers[a], David A. Leopold[b], Jeff H. Duyn[a]

PubMed

A service of the U.S. National Library and the National Institutes of Health

3: Grill HJ, Skibicka KP, Hayes MR.

Imaging obesity: fMRI, food reward, and feeding.
Cell Metab. 2007 Dec;6(6):423-5.
PMID: 18054310 [PubMed - indexed for MEDLINE]

See Lexicus. No items found.
Your search for *donuts fmri* retrieved no results.
However, a search for *donut fmri* retrieved the following items.

Neural Activation Patterns of Methamphetamine-Dependent Subjects During Decision Making Predict Relapse

Martin P. Paulus, MD; Susan F. Tapert, PhD; Mary A. Schuckit, MD

Acute effects of alcohol on neural correlates of episodic memory encoding

Hedvig Söderlund,[a,*] Cheryl L. Grady,[a,b,c] Craig Easdon,[a] and Endel Tulving[a,b]

Marketing actions can modulate neural representations of experienced pleasantness

Hilke Plassmann*, John O'Doherty*, Baba Shiv†, and Antonio Rangel*‡

Mapping a multidimensional emotion in response to television commercials

Jon D. Morris [1 2 *], Nelson A. Klahr [2 3], Feng Shen [1], Jorge Villegas [1], Paul Wright [2 3], Guojun He [2 3], Yijun Liu [2 3 *]

Hippocampal Activation for Autobiographical Memories over the Entire Lifetime in Healthy Aged Subjects: An fMRI Study

Distinguishing specific sexual and general emotional effects in fMRI—Subcortical and cortical arousal during erotic picture viewing

Martin Walter,[a,*] Felix Bermpohl,[b] Harold Mouras,[c] Kolja Schiltz,[a,d] Claus Tempelmann,[d] Michael Rotte,[d] Hans Jochen Heinze,[d] Bernhard Bogerts,[a] and Georg Northoff[a]

Cabernet and fMRI

1050–1054 | PNAS | January 22, 2008 | vol. 105 | no. 3

Marketing actions can modulate neural representations of experienced pleasantness

Hilke Plassmann*, John O'Doherty*, Baba Shiv†, and Antonio Rangel*‡

*Division of the Humanities and Social Sciences, California Institute of Technology, MC 228-77, Pasadena, CA 91125; and †Stanford Graduate School of Business, Stanford University, 518 Memorial Way, Littlefield L383, Stanford, CA94305

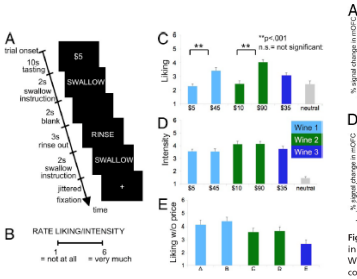

Fig. 1. Experimental design and behavioral results. (*A*) Time course for a typical trial. (*B*) Reported pleasantness and intensity rating scales. (*C*) Reported pleasantness for the wines during the cued price trials. (*D*) Taste intensity ratings for the wines during the cued price trials. (*E*) Reported pleasantness for the wines obtained during a postexperimental session without price cues.

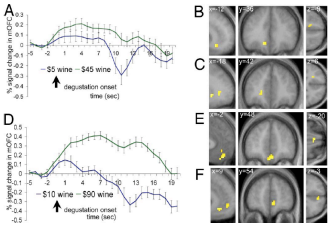

Fig. 2. The effect of price on each wine. (*A*) Wine 1: averaged time courses in the medial OFC voxels shown in *B* (error bars denote standard errors). (*B*) Wine 1: activity in the mOFC was higher for the high- ($45) than the low-price condition ($5). Activation maps are shown at a threshold of $P < 0.001$ uncorrected and with an extend threshold of five voxels. (*C*) Wine 1: activity in the vmPFC was also selected by the same contrast. (*D*) Wine 2: averaged time courses in the medial OFC voxels shown in *E*. (*E*) Wine 2: activity in the mOFC was higher for the high- ($90) than for the low-price condition ($10). (*F*) Wine 2: activity in the vmPFC was higher for the same contrast.

Resting-State fMRI

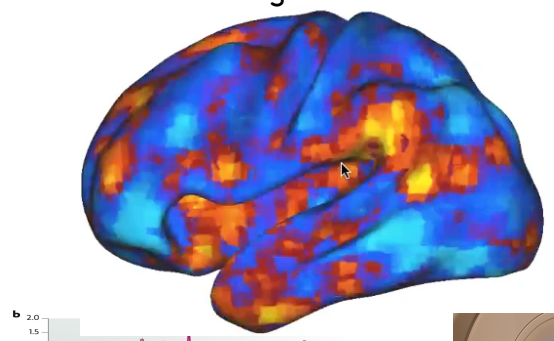

http://www.youtube.com/watch?v=VaQ66IDZ-08&feature=plcp

Resting-State BOLD Connectivity

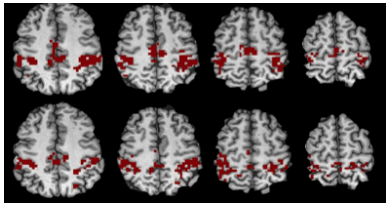

Task-Related
Motor Activation Map

Resting State Correlation Map

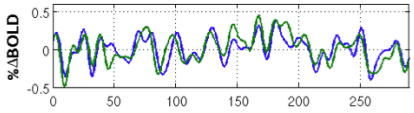

Resting State fMRI Signals From Left and Right Motor Cortices

Default Mode and Attention Networks

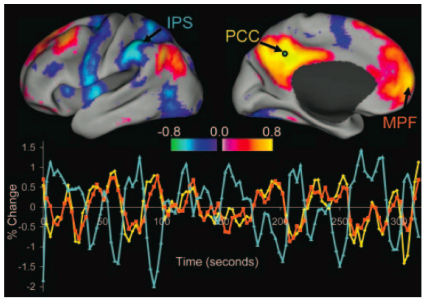

Fig. 1. Intrinsic correlations between a seed region in the PCC and all other voxels in the brain for a single subject during resting fixation. The spatial distribution of correlation coefficients shows both correlations (positive values) and anticorrelations (negative values), thresholded at $R = 0.3$. The time course for a single run is shown for the seed region (PCC, yellow), a region positively correlated with this seed region in the MPF (orange), and a region negatively correlated with the seed region in the IPS (blue).

Gusnard et al, Nat Rev. Neuro, 2001; Fox et al, PNAS 2005

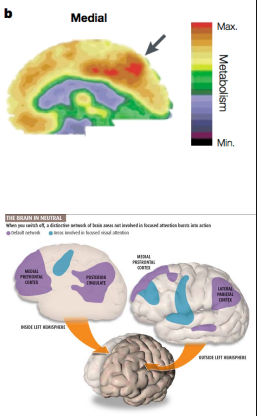

http://www.newscientist.com/data/images/archive/2681/26811501.jpg

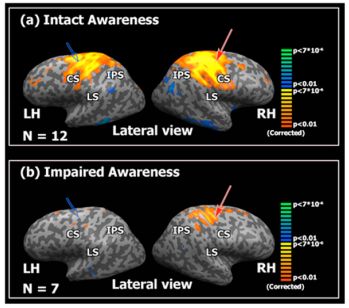

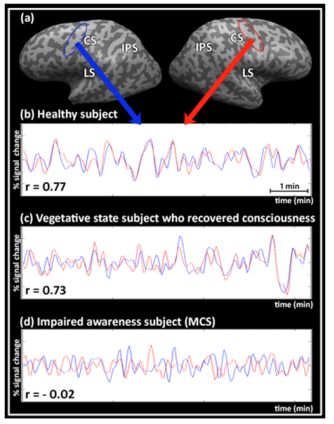

Ovadia-Caro S, Nir Y, Soddu A, Ramot M, et al. (2012) Reduction in Inter-Hemispheric Connectivity in Disorders of Consciousness. PLoS ONE 7(5): e37238. doi:10.1371/journal.pone.0037238
http://www.plosone.org/article/info:doi/10.1371/journal.pone.0037238

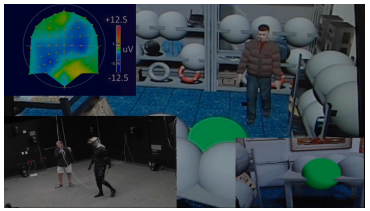

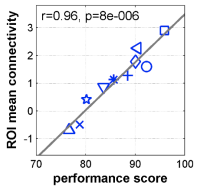

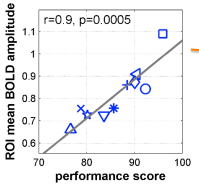

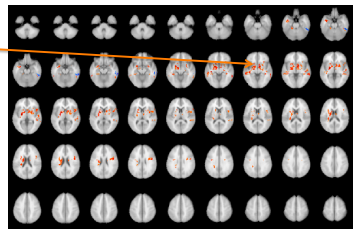

video courtesy of Howard Poizner

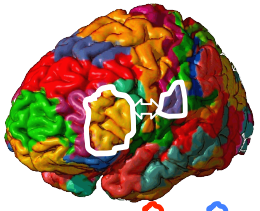

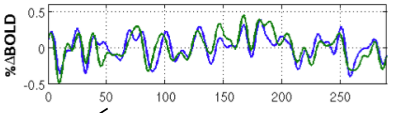

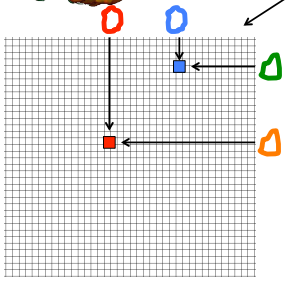

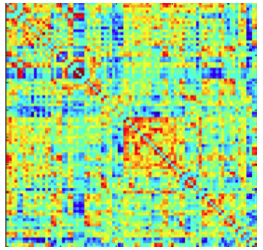

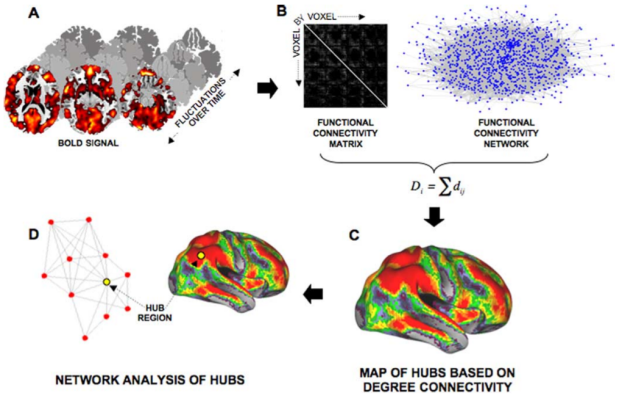

Figure 1. Methods for identifying cortical hubs and networks. *A*, The basis of the present methods is the intrinsic BOLD signal fluctuations that correlate between brain regions reflecting monosynaptic and polysynaptic connections. *B*, The functional connectivity matrix was computed to represent the strength of correlation between every pair of voxels across the brain; the pattern of these connections is the functional connectivity network (example is of a binary matrix and network of 1000 nodes). *C*, To determine cortical hubs, the degree of connectivity of each voxel was computed and projected onto the cortical surface of the brain. Candidate hubs are those regions with disproportionately high connectivity and are plotted in yellow and red. *D*, As a secondary analysis, the networks associated with identified hubs were determined by seeding individual regions located at the peak of the hub and determining the subnetworks that showed correlation.

Buckner et al, J. Neuroscience, 2009

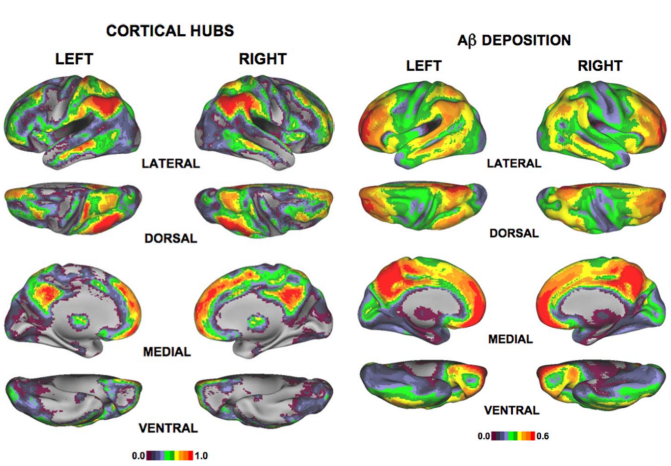

Buckner et al, J. Neuroscience, 2009

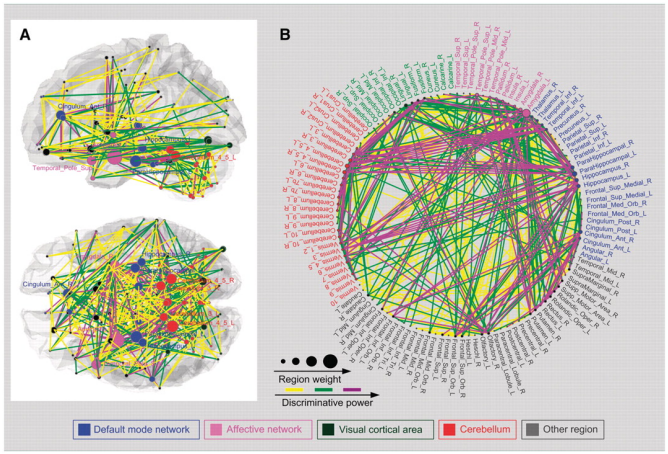

Zeng L et al. Brain 2012;135:1498-1507

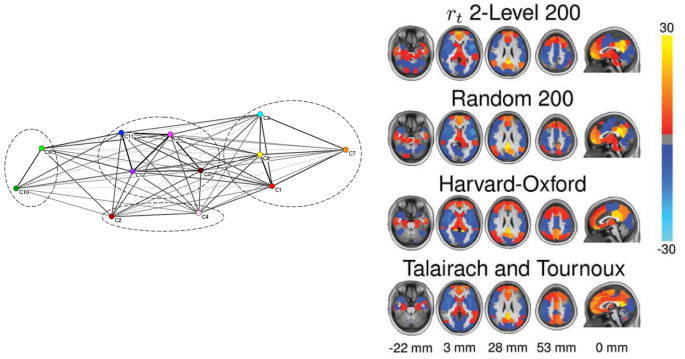

Goulas et al, Jneuroscience, 2012

Craddock et al, HBM 2012

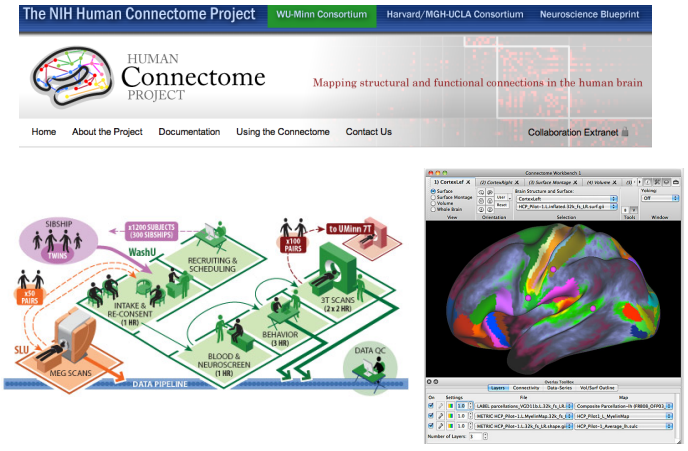

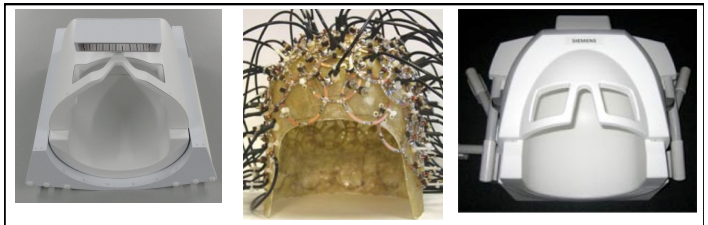

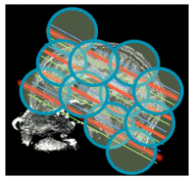

Connectome Protocol:
8 simultaneous slices
2 mm isotropic resolution
TR 720 ms; TE = 32 ms

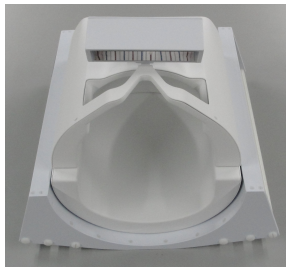

Nova 32 channel

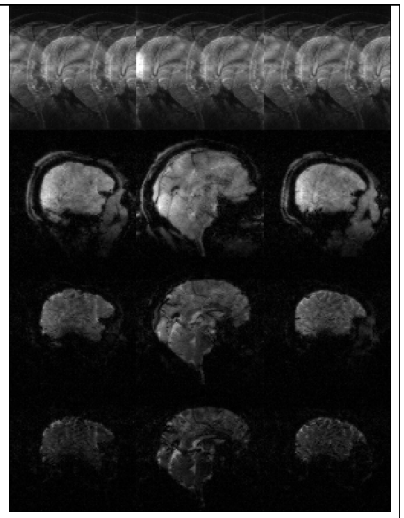

Real-Time fMRI

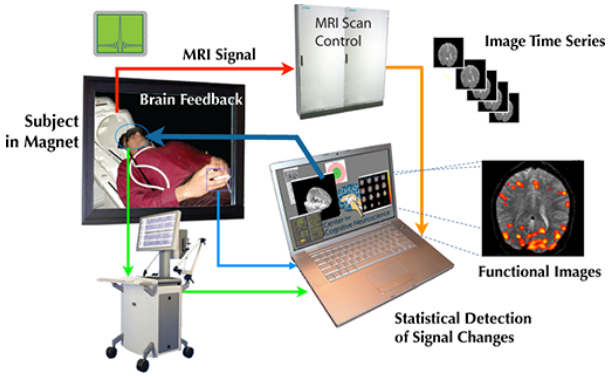

http://www.brainmapping.org/MarkCohen/research/RTfMRI.html

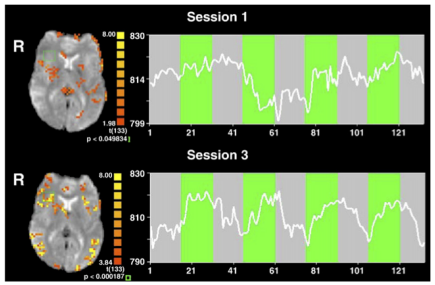

Fig. 3. Single subject statistical maps (left) and BOLD time-courses (right) of the right anterior insula in the first (top) and in the last session (bottom). The selected region of interest is delineated by the green box. Functional images are in the radiological convention and are not normalized. Statistical significance was based on *t* test comparing activation on each voxel during the regulation blocks with respect to the baseline blocks, with a threshold of $P<0.05$ false discovery rate (FDR) corrected for multiple comparisons (Genovese et al., 2002). The time course of the BOLD activity (white line) is related to the ROI selected and is showing the progress during the regulation blocks (green) and the baseline blocks (gray). Number of volumes is in the *x* axis and magnitude signal in the *y* axis; these values are the raw output from the scanner.

Caria et al, NIMG 2007

Timeline

Michael Crichton, 1999

"Most people", Gordon said, "don't realize that the ordinary hospital MRI works by changing the quantum state of atoms in your body ... But the ordinary MRI does this with a very powerful magnetic field - say 1.5 tesla, about twenty-five thousand times as strong as the earth's magnetic field. We don't need that. We use Superconducting QUantum Interference Devices, or SQUIDs, that are so sensitive they can measure resonance just from the earth's magnetic field. We don't have any magnets in there".

J. Clarke, UC Berkeley

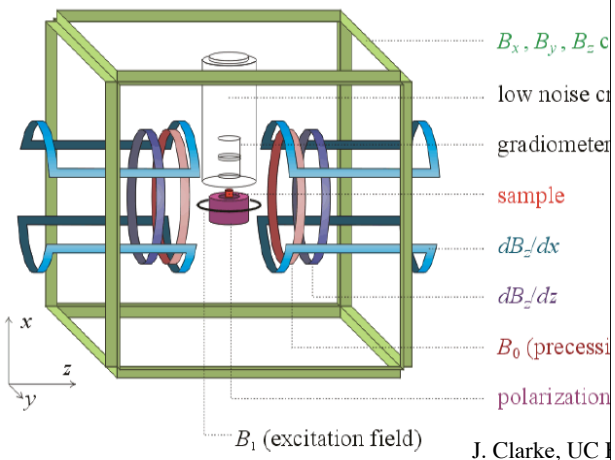

J. Clarke, UC

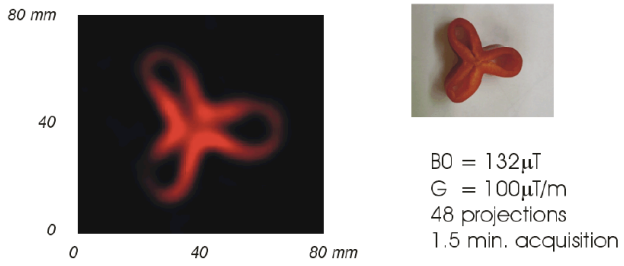

J. Clarke, UC Berkeley

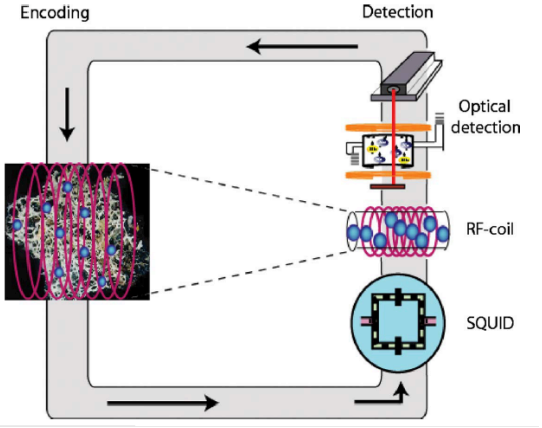

Seeley et al, JMR 2004

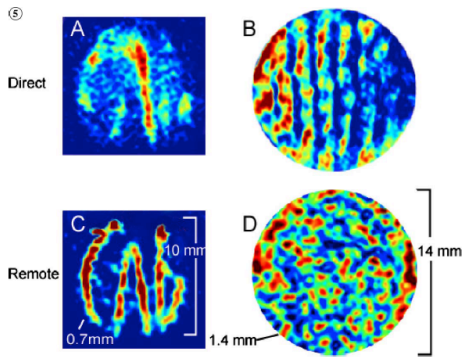

Seeley et al, JMR 2004

Compressed Sensing

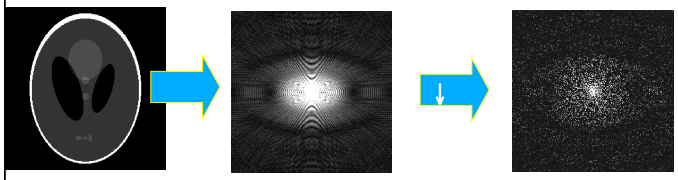

Slide Credit: http://www.stanford.edu/~mlustig/

Compressed Sensing

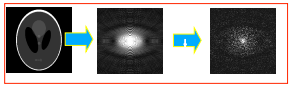

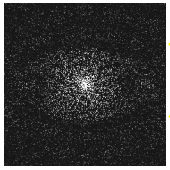

Minimum - norm conventional linear reconstruction

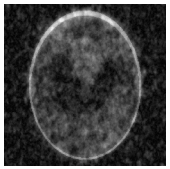

Min. Total Variation (TV) A convex non-linear reconstruction

Slide Credit: http://www.stanford.edu/~mlustig/